

## The QCD EoS from simulations on BlueGene L Supercomputers at LLNL and NYBlue

---

**Rajan Gupta\*** (HotQCD Collaboration<sup>†</sup>)

*Theoretical Division, Los Alamos National Laboratory, Los Alamos, NM 87545, USA*

*E-mail: [rajan@lanl.gov](mailto:rajan@lanl.gov)*

We present results for the QCD Equation of State (EoS) obtained using simulations of lattice QCD at zero chemical potential. Our high statistics results compare improved asqtad and p4fat3 staggered quarks on lattices with a temporal extent  $N_\tau = 6$  and 8 and light quark masses approximately one fifth and one tenth the strange quark mass. We find that the two actions give consistent results and estimate that the trace anomaly  $(\epsilon - 3p)/T^4$  obtained on  $N_\tau = 8$  lattices represents the continuum value to better than 20% uncertainty over the temperature range 140 – 700 MeV. The precision in the estimates of energy density and pressure are better, therefore, we conclude that lattice estimates of the energy density and pressure should be used in the phenomenological analysis of RHIC and LHC data. We also find a consistent picture of the crossover temperature from all observables studied, with the best estimated range to be 185 – 195 MeV. These calculations are being carried out on the IBM BlueGene/L supercomputer at Lawrence Livermore National Laboratory and at the New York Center for Computational Science (NYBlue).

*The XXVI International Symposium on Lattice Field Theory*

*July 14-19 2008*

*Williamsburg, Virginia, USA*

---

\*Speaker.

<sup>†</sup>Alexei Bazavov, Tanmoy Bhattacharya, Michael Cheng, Norman Christ, Carleton DeTar, Steven Gottlieb, Rajan Gupta, Urs Heller, Kay Huebner, Chulwoo Jung, Frithjof Karsch, Edwin Laermann, Ludmila Levkova, Thomas Luu, Robert Mawhinney, Peter Petreczky, Dwight Renfrew, Christian Schmidt, Ron Soltz, Wolfgang Soeldner, Robert Sugar, Doug Toussaint, and Pavlos Vranas

## 1. Introduction

Experiments at the Brookhaven Relativistic Heavy Ion Collider (RHIC), and at the LHC, will study the formation and evolution of the quark gluon plasma. The phenomenological analysis of the data has relied on a hydrodynamic description of the medium, and the results suggest a strongly interacting plasma with very small viscosity. A crucial input (and eventually the goal) of this phenomenological analysis is the characterization of the equation of state (EoS) over the temperature range 140 – 700 MeV relevant to experiments at both RHIC and LHC. Theoretically, simulations of Lattice QCD provide a first principles analysis of QCD in the vicinity of thermal equilibrium and zero baryon and strangeness chemical potential (For recent reviews see [1, 2]). The results of our detailed analysis of the equation of state as a function of temperature will, therefore, provide crucial guidance in the phenomenological interpretation of experimental measurements.

A related quantity of high interest is the transition temperature from hadrons to a quark-gluon plasma (QGP). The minimum energy density required to produce a quark-gluon plasma grows as the fourth power of the temperature. Thus, a 10% error in the threshold temperature corresponds to a 45% error in the threshold energy density. Previous calculations with staggered fermions have found the transition for 2 + 1 flavors to be a rapid crossover. In light of this lack of a true phase transition (see, for example, [3]), we will discuss what quantities to focus on for estimating the transition temperature needed in the phenomenological analysis of heavy ion collisions.

This talk updates the status of HotQCD results for the EoS and the transition temperature obtained from large scale simulations on the BlueGene L at LLNL and NYCCS (NYBlue) [4, 1, 2]. These calculations have been carried out with two sets of  $\mathcal{O}(a^2)$  improved actions, asqtad and p4fat3 staggered fermions, and for each of these actions we have simulated on lattices with extent  $N_\tau = 6$  and 8 in the Euclidian time direction and a spatial extent of  $32^3$ . The strange quark mass is fixed to roughly the physical strange quark value, and  $m_l/m_s = 0.1$  and 0.2 corresponding to Goldstone  $M_\pi \approx 215$  and 304 MeV. For preliminary results at  $m_\ell = 0.05m_s$  see talk by Soeldner [6]. The associated  $T = 0$  calculations needed to subtract ultraviolet divergences in the EoS and determine the lattice spacing were done on  $32^4$  or larger lattices. We discuss uncertainties associated with the continuum and chiral extrapolations based on these combined data sets.

## 2. Parameter Sets Used in the Simulations

The run parameters for simulations with the p4fat3 action are given in Table 1, and those for the asqtad action in Table 2. The lattice scale is set using  $r_0$  (or equivalently  $r_1$  as they give consistent estimates). The simulations are being carried out along lines of constant physics by adjusting the bare strange quark mass to produce an approximately constant physical value of  $M_{\bar{s}s} = 686$  MeV corresponding to  $M_{\bar{s}s}r_0 = 1.58$  and  $M_\pi r_0 \approx 0.52$  for  $M_\ell = 0.1m_s$  along the trajectory. Having fixed the strange quark mass we are simulating three light quark mass values held fixed at  $m_\ell/m_s = 0.2, 0.1$  and 0.05. To allow comparison with previous studies the asqtad trajectory in HotQCD simulations is set 20% higher than the physical strange quark mass.

## 3. Strategy for Precision Calculations

Our goal is to map out the EoS over the temperature range 140-700 MeV to within 5% uncer-

$N_\tau$	$N_s$	$m_\ell/m_s$	Total # of $\beta$ values	Independent Streams	Total # trajectories per $\beta$ (0.5 length)
6	16	0.2	9	RBC-Bielefeld	10-60K
6	16	0.1	8	RBC-Bielefeld	25-60K
	24			Collaboration [5]	5-8K
8	32	0.2	7	2	14-15K
8	32	0.1	30	1 – 3	8-37K
32	32	0.1	21	1	2-6K

**Table 1:** Simulation parameters for the p4fat3 action. For thermalization 800 trajectories are discarded. We also indicate the number of independent streams used to accumulate statistics.

$N_\tau$	$N_s$	$m_\ell/m_s$	Total # of $\beta$ values	Independent Streams	Total # trajectories per $\beta$ (unit length)
6	32	0.2	7	1	18-20K
6	32	0.1	7	1	18-19K
8	32	0.2	8	1	13K
8	32	0.1	23	1	15-16K
8	64	0.1	1	1	3.7K
32	32	0.1	18	1	5-6K

**Table 2:** Simulation parameters for the asqtad action. 1000-1200 time units are discarded for thermalization.

tainty. In addition to performing high statistics simulations (see Tables 1 and 2) we have adopted the following strategy to understand and control systematic errors.

1. Discretization Errors: We are simulating two improved staggered actions – asqtad and p4fat3 – that have different  $O(a^2)$  errors. This provides a check but does not address the rooting issue for staggered fermions.
2. Continuum Limit: Our goal is to perform a continuum extrapolation along lines of constant physics using lattices with  $N_\tau = 6, 8$  and  $12$ .
3. Extrapolation to physical  $u, d$  quark masses and the chiral limit will be done using  $m_\ell/m_s = 0.2, 0.1$  and  $0.05$ . Staggered taste violations in finite  $T$  calculations require resolving what effective  $M_\pi$  should correspond to these quark masses and thus the physical value of  $m_{u,d}$  [1].
4. Crossover Temperature: Recognizing the absence of a phase transition at physical values of the quark masses, we are simulating at  $2 - 5$  MeV interval over the entire crossover region to provide a precise quantitative picture of the transition in energy density, pressure, etc.
5.  $T = 0$  simulations needed for performing subtractions of lattice artifacts in the determination of the EoS: We are simulating almost as many  $\beta$  values ( $\approx 20$  for each action at  $N_\tau = 8$ ) as used in finite temperature runs. Estimates of  $a$  includes the much larger asqtad zero-temperature program.

#### 4. Equation of State

Our preliminary results for the trace anomaly ( $(\varepsilon - 3p)/T^4$ ) for both actions and for  $N_\tau = 6$  and 8 lattices are shown in Fig. 1. Over the full range  $T = 140 - 500$  MeV, we find the same pattern for both actions on going from  $N_\tau = 6$  to 8, *i.e.* a decrease in peak height and a slight shift of points to lower  $T$ , with the largest change in the range  $T = 190 - 300$  MeV. A more detailed picture of the data over  $(140 \leq T \leq 200)$  MeV is also presented in Fig. 1 (right figure), and in Fig. 2 for  $(180 \leq T \leq 300)$  MeV (left figure), and  $(300 \leq T \leq 700)$  MeV (right figure).

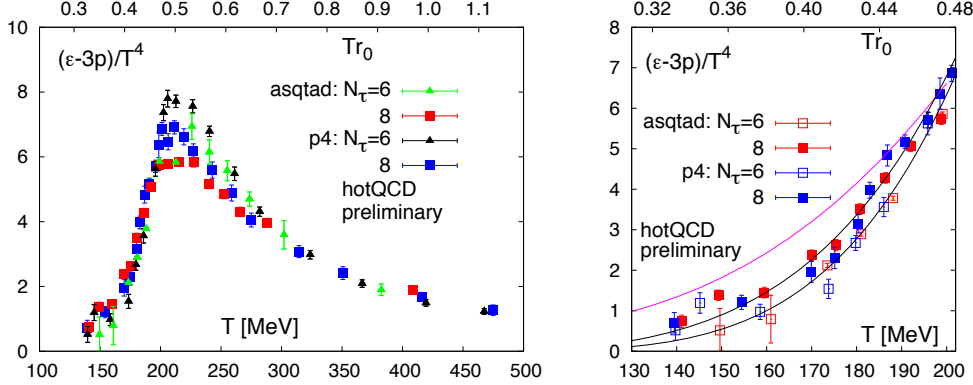


**Figure 1:** Preliminary results for the trace anomaly for the p4fat3 and asqtad actions as a function of temperature in MeV and in units of  $r_0$ . The figure on the right magnifies the range  $T = 140 - 200$  MeV and includes fits to the p4fat3 points. The purple curve above the data is from the hadron resonance gas model.

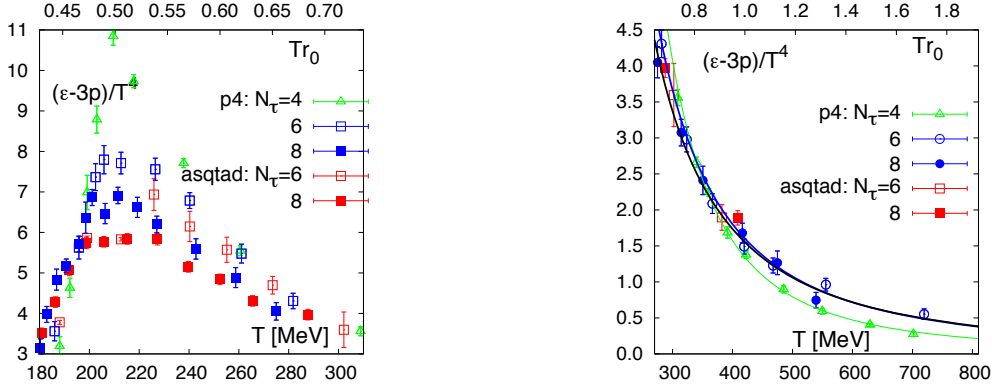


**Figure 2:** Details of EoS data for the p4fat3 and asqtad actions. The left figure shows the range  $T = 180 - 300$  MeV and the right figure shows the range  $T = 300 - 700$  MeV and fits to the p4fat3 data.

Data in the range  $T = 140 - 200$  MeV lie below the hadron resonance gas (HRG) model. There is an upward shift (larger value of  $(\varepsilon - 3p)$ ) on going from  $N_\tau = 6$  to 8, which for some of the points is comparable to the difference between the  $N_\tau = 8$  data and the HRG estimate.

The discretization effects are most pronounced in the range  $T = 180 - 300$  MeV. We find up to 20% decrease in the peak on going from  $N_\tau = 6$  to 8 for both actions and the asqtad data lie below p4fat3 values by up to 15%. We find that the position of the peak remains above 200 MeV, as already observed in the  $N_\tau = 4$  data with p4fat3 action [2, 4].

At higher temperatures ( $T > 300$  MeV) the  $N_\tau = 6$  and 8 data are consistent. There, however, are two unresolved issues. The first is possible finite volume effects at  $T > 400$  MeV. The one  $N_\tau = 8$  asqtad point at  $T = 400$  MeV on  $64^3$  lattices is consistent with those on  $32^4$  lattices, however, more data are needed at  $T > 300$  MeV. Second, when fitting the data using the expected  $c_0 + c_2/T^2 + c_4/T^4$  form, the running of the QCD coupling requires the asymptotic behavior to have a  $g^4$  variation in  $c_0$ . Current data are not good enough to resolve this feature.

Overall, our preliminary results provide a reasonably consistent picture of the EoS over the full temperature range and are of sufficient precision to be incorporated into hydrodynamical models. The current uncertainty of up to 20% at 180 – 300 MeV in the trace anomaly is expected to reduce to roughly 5% with inclusion of data at  $m_\ell/m_s = 0.05$  and new simulations on  $N_\tau = 12$  lattices.

## 5. Entropy Density Across the Transition

The energy and entropy densities are two very useful markers of the crossover temperature as these are the quantities that enter into the phenomenological analyses of heavy ion collisions.

The data for energy density  $\varepsilon$ , pressure  $p$ , and the entropy density  $s/T^3 = (\varepsilon + p)/T^4$  are shown in Fig. 3. We observe a rapid cross-over in the range 175 – 205 MeV and a smaller difference between  $N_\tau = 6$  and 8, and conclude that quarks and gluons become the dominant and relevant degrees of freedom above 250 MeV, a region that will be probed at the LHC.

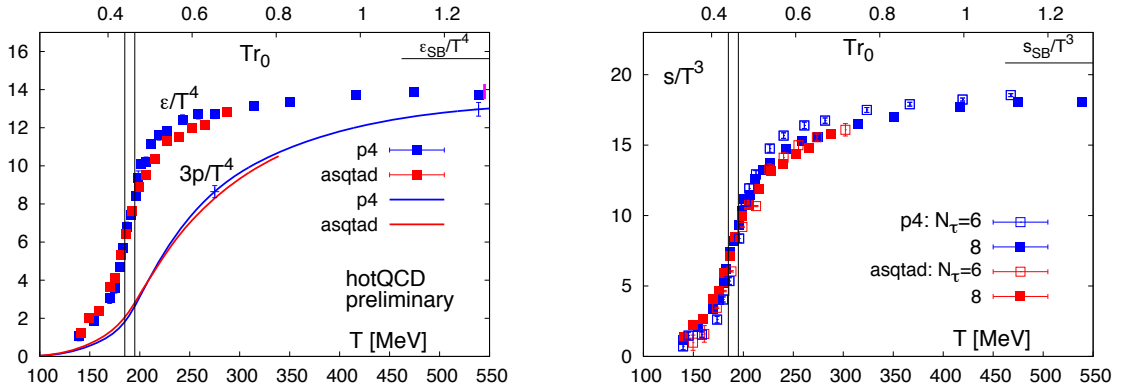


**Figure 3:** Results for energy, pressure and entropy density for the p4fat3 and asqtad actions with  $m_\ell/m_s = 0.1$  over  $T = 140 - 550$  MeV. The band  $T = 185 - 195$ , drawn to guide the eye, covers the inflection point.

## 6. Deconfinement and Chiral Transitions

This section summarizes results for quantities used to probe the deconfinement (Polyakov loop and quark number susceptibility) and the chiral (chiral condensate and its susceptibility) transitions.

The data for the renormalized Polyakov loop  $\langle L_{\text{ren}}(T) \rangle = Z(g^2)^{N_\tau} \langle L_{\text{bare}}(T) \rangle$ , which measures the free energy  $F_\infty$  of an isolated quark,  $L_{\text{ren}} = \exp[-F_\infty(T)/(T)]$ , is shown in Fig. 4. There is a small,  $< 10\%$ , difference between p4fat3 and asqtad data above  $T = 200$  MeV with the general trend that the difference decreases with increasing  $N_\tau$ . The continued slow rise beyond  $T \sim 250$  MeV results in a broad shoulder past the peak in the associated susceptibility, and by  $N_\tau = 8$  there

no longer is a well defined inflection point (in  $L_{\text{ren}}$ ) nor a peak in its susceptibility. We find that locating the transition  $T$  from the inflection point in  $L_{\text{ren}}$  is already marginal at  $N_\tau = 6$  [5].

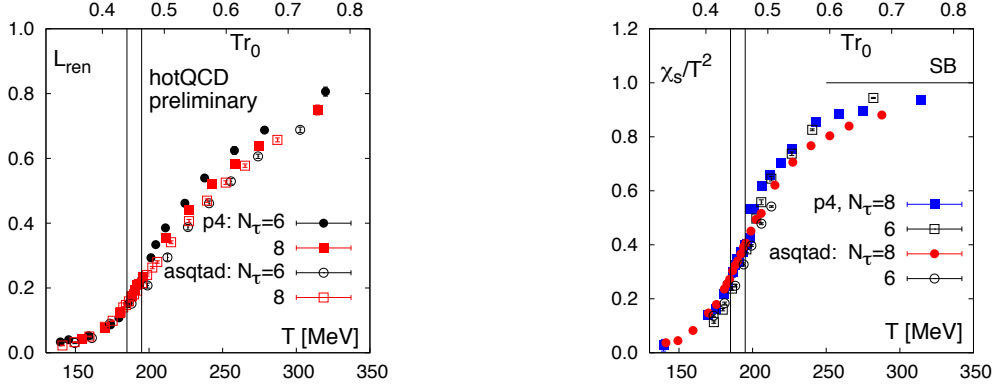


**Figure 4:** Deconfinement indicators for p4fat3 and asqtad actions. (A) Renormalized Polyakov loop. (B) Strange quark number susceptibility  $\chi_s/T^2$ . The band 185 – 195 MeV captures the inflection point.

P4fat3 and asqtad data for the strange quark number susceptibility,  $VT\chi_s = \partial \ln Z / \partial^2 (\mu_s/T)$ , are shown in Fig. 4. They are consistent for both  $N_\tau = 6$  and 8 and show a rapid crossover with the inflection point covered by the band at 185 – 195 MeV.  $\chi_s$  is a good probe of deconfinement as it measures fluctuations in the strange charge and therefore it does not need renormalization. The location of the peak in the fluctuations, however, requires calculating the fourth derivative, which is still in progress.

The chiral condensate is investigated using the combination

$$\Delta_{l,s}(T) = \frac{\langle \bar{\psi}\psi \rangle_\ell(T) - m_\ell/m_s \langle \bar{\psi}\psi \rangle_s(T)}{\langle \bar{\psi}\psi \rangle_\ell(0) - m_\ell/m_s \langle \bar{\psi}\psi \rangle_s(0)} \quad (6.1)$$

in which the additive ultraviolet divergence of the form  $m/(a^2)$  at nonzero quark mass is removed. The data in Fig. 5 show consistency between the two actions by  $N_\tau = 8$  indicating that the residual different additive and multiplicative renormalization factors due to slight differences in the lattice parameters between the two actions mostly cancel in  $\Delta_{l,s}(T)$ . The difference between  $N_\tau = 6$  and 8 data are mostly accounted for by shifting the  $T$  of  $N_\tau = 6$  data to the left by  $\approx 5$  MeV. Lastly, the inflection point in the crossover is again captured by the band at 185 – 195 MeV.

Fluctuations in the light quark condensate are given by the isosinglet chiral susceptibility. It consists of the connected and disconnected parts  $\chi_{\text{singlet}} = \chi_{\text{disc}} + 2\chi_{\text{conn}}$ . Data for  $\chi_{\text{disc}}$  for the two actions on  $N_\tau = 8$  lattices are compared in Fig. 5 and exhibit four features. (A) Consistency between the two actions; (B) an increase in peak height with decreasing quark mass; (C) A shift by  $\sim 10$  MeV towards smaller  $T$  between  $m_\ell/m_s = 0.2$  and 0.1; and (D) a broadening of the peak as  $m_q \rightarrow 0$ . Karsch [7] has argued that, below the transition in the broken chiral symmetry phase, fluctuations caused by the vanishing Goldstone pion mass should broaden the peak, *i.e.*,  $\chi_{\text{singlet}} \rightarrow \infty$  with  $m_q \rightarrow 0$  for all  $T \leq T_c$ . If this picture (consistent with our data) is substantiated then the location of the right edge of this broad peak would be the appropriate locator of the chiral symmetry restoration temperature. Extrapolating this edge, using our  $m_\ell/m_s = 0.1$  and 0.2 data, to the chiral limit gives  $T_{\text{transition}} > 180$  MeV for  $N_\tau = 8$ .

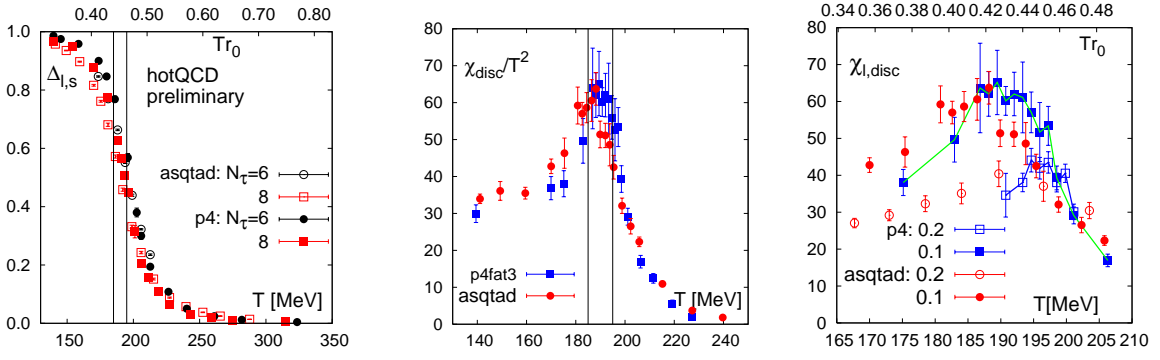


**Figure 5:** P4fat3 and asqtad data for the chiral symmetry restoration transition: (Left) The subtracted condensate  $\Delta_{l,s}$ ; (Center)  $\chi_{disc}$  for  $m_\ell = 0.1m_s$ ; (Right) Comparison of peak in  $\chi_{disc}$  with  $m_\ell/m_s = 0.1$  and  $0.2$ . Note the broadening of the peak and strong  $m_{quark}$  dependence attributed to Goldstone modes [7].

## 7. Conclusions

Data for  $(\varepsilon - 3p)/T^4$  show consistency between asqtad and p4fat3 actions and exhibit  $< 20\%$  change between  $N_\tau = 6$  and  $8$ . We consider estimates of  $\varepsilon$  and  $p$  on  $N_\tau = 8$  lattices are precise enough to use in phenomenological analyses of the evolution of the QGP at RHIC ( $T < 300$  MeV).

All observables used to probe the transition (energy and entropy density, Polyakov loop, quark number susceptibility, chiral condensate and its susceptibility) show a rapid crossover that takes place between  $175 \leq T \leq 205$  MeV with  $185 - 195$  MeV as our best estimate for the transition temperature most relevant for phenomenological studies.

These calculations are being extended in two ways. First, simulations are being done at  $m_\ell = 0.05m_s$  to directly probe the system at approximately the physical  $u, d$  mass [6]. Second, for continuum extrapolation we plan to simulate  $N_\tau = 12$  lattices in addition to  $N_\tau = 6$  and  $8$ .

## Acknowledgments

We are grateful to LLNL, NNSA, and New York Center for Computational Science for providing access to the Bluegene/L supercomputers. This work is supported by US DOE and NSF.

## References

- [1] C. DeTar, *Recent Progress in Lattice QCD Thermodynamics*, PoS (LAT2008)
- [2] F. Karsch, *Recent lattice results on finite temperature and density QCD*, PoS (LAT2007)015.
- [3] Y. Aoki, Z. Fodor, S. D. Katz and K. K. Szabo, *The QCD transition temperature: Results with physical masses in the continuum limit*, Phys. Lett. B **643** (2006) 46 [arXiv:hep-lat/0609068].
- [4] C. DeTar, R. Gupta [HotQCD Collaboration], *Towards a precise determination of  $T_c$  with 2+1 flavors of quarks*, PoS (LAT2007) 179 [arXiv:hep-lat/0710.1655].
- [5] M. Cheng, *et al*, *The Transition Temperature in QCD*, Phys. Rev. D **74** (2006) 054507.
- [6] W. Soeldner, *Quark mass dependence of the QCD EoS on  $N_t=8$  lattices*, PoS (LAT2008)
- [7] F. Karsch, *Fluctuations of Goldstone modes and the chiral transition in QCD*, SEWM 2008.